Conceptual design of a rotational mechanical time base with varying inertia

E. Thalmann* S. Henein†

Article history

June 4, 2019: Submitted.
August 28, 2020: Revised Eq. (3) and Eq. (6)-(10).

Abstract

Flexure pivot oscillators have the potential to advantageously replace the traditional balance wheel-spiral spring oscillator used in mechanical watches due to their significantly lower friction. However, they have inherent nonlinear elastic properties that can introduce a variation of their frequency with amplitude called isochronism defect. Previous research has focused on controlling the elastic behavior of flexure pivot oscillators to reach isochronism. We present a new way of minimizing the isochronism defect of rotational oscillators by varying their inertia. This principle is embodied in a new family of oscillators we call rotation-dilation coupled oscillator (RDCO). Their architecture also presents a rotational symmetry that is advantageous for minimizing the effects of gravity on their period. We present a description of this new oscillator family, give conceptual tools for tuning its isochronism and show examples of physical implementations.

1 Introduction

1.1 Isochronism

The primary goal of mechanical time bases is accurate timekeeping, which is essentially equivalent to having a period of oscillation that is as regular as possible. The key property sought by horologists to reach this accuracy is *isochronism*: the independence of oscillation period from oscillation amplitude [13, 16]. Theoretically, a simple harmonic oscillator consisting of an inertial element and a spring whose restoring force follows Hooke's law (i.e. proportional and in opposite direction to the displacement) is isochronous. Classical mechanical watches use a time base consisting of a spiral spring attached to a balance wheel rotating on jewelled bearings such as depicted in Fig. 1. The spiral spring is designed such that its restoring torque is a linear as possible, thus achieving good isochronism.

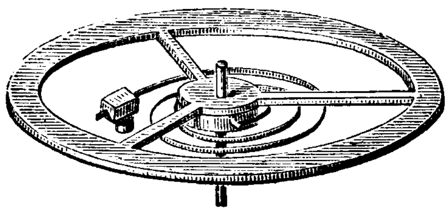

Figure 1: Classical mechanical watch time base [15].

1.2 Flexure pivot time bases

In order to increase the accuracy of mechanical watches, the consensus among horologists is that the quality factor of the oscillator must be increased [2, 13, 18]. One promising way of achieving this is to drastically reduce the friction in the pivot of the oscillator by replacing it with a flexure pivot [7]. Flexure pivots, however, often exhibit nonlinear elastic behavior which causes isochronism defect. The approach used until now was to

*Corresponding author, EPFL Instant-Lab, etienne.thalmann@epfl.ch
†EPFL Instant-Lab, simon.henein@epfl.ch

correct the restoring torque characteristic to obtain the desired isochronism. The first flexure pivot introduced in a watch in 2014 by Barrot et al. [1] used an external mechanism [10] to compensate for its nonlinearity. Alternatively, Di Domenico et al. [5] [6] [9] use crossed flexure pivots with special values for the point at which the leaf springs cross and the angle between them to obtain the desired restoring torque characteristic. In previous work, we also presented a flexure pivot whose restoring torque nonlinearity can be modified by adjusting the crossing point of the flexures while preserving its property of minimizing the effect of gravity on the stiffness [12, 17].

1.3 Inertial isochronism correction

Here, we propose to use the inertia variation of a rotational oscillator to minimize its isochronism defect. This idea is new and is the principal contribution of this article. Our goal is not only to compensate for the restoring torque nonlinearity of the oscillator but to be able to compensate any cause of isochronism defect external to the oscillator. It is indeed known that escapements introduce isochronism defects and this property has already been compensated by Henein and Schwab [10] or used to compensate the defect of pendulums in precision clocks [3, pp.33-34] [20, pp.79-80].

Our concept is analogous to the theoretical isochronism corrector for the pendulum devised by Huygens in 1656 [11]. He calculated that the restoring torque of the pendulum caused by gravity was not proportional to its displacement, which caused an isochronism defect. He proposed to compensate this defect by replacing the rod with a flexible cord which unwinds off a cycloid, as depicted in Fig. 2, which essentially corresponds to changing the active length of the pendulum as it swings. The analogy between changing the inertia J of a rotational oscillator as it rotates and changing the active length L of a pendulum as it swings can be seen from the formulas for angular frequency, namely $\sqrt{k/J}$ for a rotational oscillator of stiffness k and $\sqrt{g/L}$ for a pendulum under gravity g.

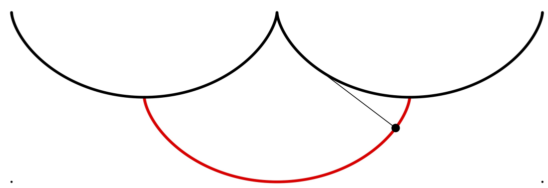

Figure 2: Huygens' isochronism correction for the pendulum by changing its active length as it oscillates [19].

It is well known that inertia variations can be used to tune the nominal frequency of rotational oscillators. This was for example implemented on marine chronometers, by changing the position of screws placed on their balance wheel [16, pp.259-262]. This concept is however different form the one proposed in this paper as it results in a modified inertia that stays constant during the entire oscillation and does not affect the isochronism defect. Inertia variations with temperature have also been used on oscillators to minimize the effect of temperature on frequency. This was for example implemented on marine chronometers with bimetallic balance wheels [16, pp.259-262]. Again, this inertia variation does not depend on oscillation amplitude and cannot be used to correct isochronism defects.

1.4 Structure of the paper

We present a new family of rotational oscillators called *rotation-dilation coupled oscillator* (RDCO) depicted in Fig. 3 whose inertia changes as it rotates. We give a conceptual description of the behavior of this oscillator and provide insight on how its inertia variation can be combined to its restoring torque nonlinearity to minimize its isochronism defect.

In Sec. 2, we introduce the design of the RDCO and its kinematics. We describe the crucial parameter influencing its dilation. In Sec. 3 we present a flexure implementation of the RDCO. In Sec. 4, we give the theoretical basis necessary for understanding the effect of varying inertia and nonlinear restoring torque on isochronism. We analyze the restoring torque nonlinearity of the system and give examples of configurations where this nonlinearity can be compensated by the variation of inertia.

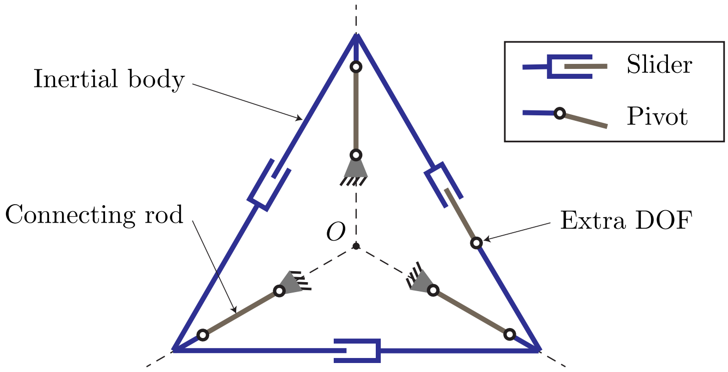

Figure 3: Kinematic diagram of the rotation-dilation coupled system.

2 Design and kinematics

2.1 Design

Figure 3 shows a kinematic diagram of the rotation-dilation coupled system. The mechanism consists of $n \geqslant 3$ inertial bodies linked to each other by sliders (prismatic joints) to form a loop ($n = 3$ in Fig. 3). Each rigid body is linked to the ground by a connecting rod with a pivot at both extremities, one connected to the inertial body and the other to the ground. The joints are placed such that they have rotational symmetry of order n with respect to the center O of the system. An extra degree-of-freedom (DOF) is added by allowing a pivoting motion in one of the sliders, see Fig. 3. The sole purpose of this extra DOF is to avoid overconstraining the system;[1] it is not activated during its motion.

2.2 Rotation-dilation coupling

The kinematic behavior of the system is determined by the dimensionless ratio $\delta = d/L$, where d and L are described in Fig. 4. We define d as the distance from the center O of the system to the axis A of the pivot connecting the connecting rod to the ground. We define L as the distance from axis A to the axis B of the second pivot of the connecting rod. The signs of d and L are defined with respect to the direction from O to B, represented by axis y in Fig. 4. Note that in most figures, the extra DOF is neglected to simplify the representations.

We classify the RDCO architectures according to three domains of the parameter δ, summarized in Fig. 4 and Table 1.

(a) When $\delta > 0$, d and L are of same sign. The connecting rods are connected to the ground between the inertial loop and point O.

(b) When $-1 < \delta < 0$, d and L are of opposite sign and $d < L$. The connecting rods cross each other inside of the inertial loop.

(c) When $\delta < -1$, d and L are of opposite sign and $d > L$. The connecting rods are connected to the ground outside of the inertial loop.

Figure 5 shows the motion of the system as it is displaced from its rest position. We call this motion *rotation-dilation coupling*, where the rotation is defined by the angle θ swept by a vector from the center O to a point P on the inertial body and the dilation is defined by the change of length of this vector. As shown in Table 1, the parameter δ influences this dilation:

- When $\delta > 0$, $\left\|\overrightarrow{OP(\theta)}\right\| < \left\|\overrightarrow{OP(0)}\right\|$ and the inertial bodies move towards each other. We call it a *negative dilation*.
- When $\delta < 0$, $\left\|\overrightarrow{OP(\theta)}\right\| > \left\|\overrightarrow{OP(0)}\right\|$ and the inertial bodies move away from each other. We call it a *positive dilation*.

[1] A mechanism is overconstrained when its mobility obtained through Grübler's formula [8] is less than its actual degree of freedom. This can lead to unpredictable variations of the stiffness of flexure mechanisms and give rise to important stresses in their flexures [4].

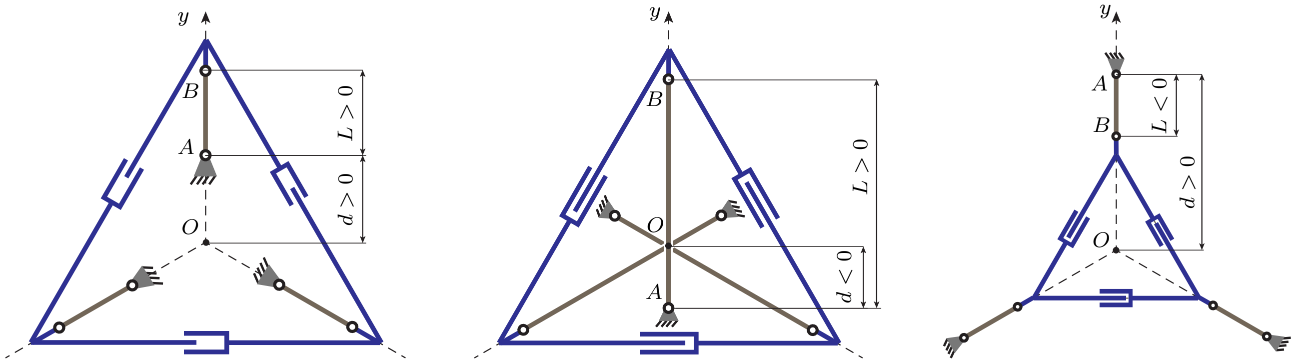

(a) $\delta > 0$ (b) $-1 < \delta < 0$ (c) $\delta < -1$

Figure 4: Defintions of d, L and $\delta = \frac{d}{L}$.

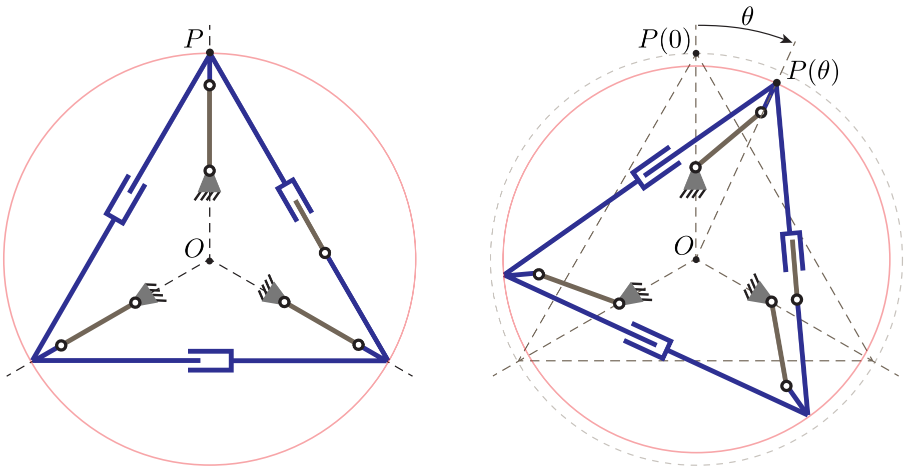

Figure 5: Rotation-dilation coupling.

	(a) $\delta > 0$	(b) $-1 < \delta < 0$	(c) $\delta < -1$
Nominal position	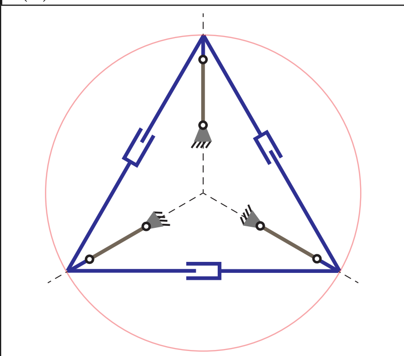	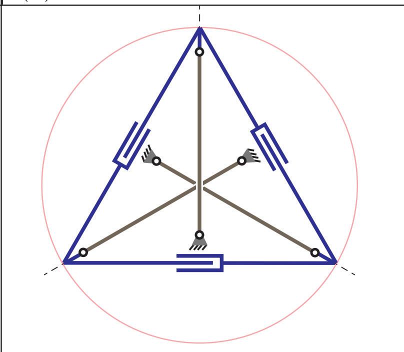	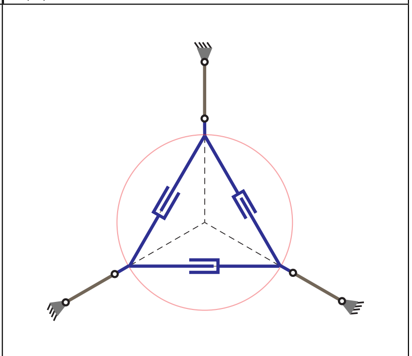
Rotated	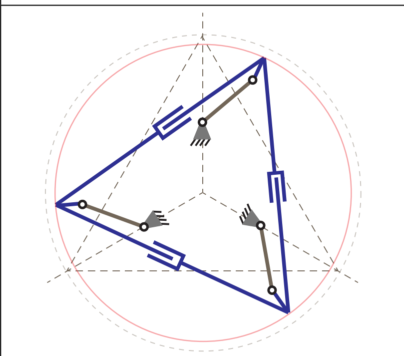	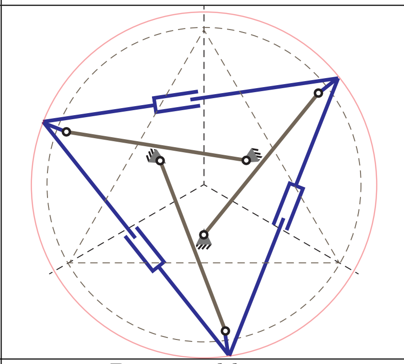	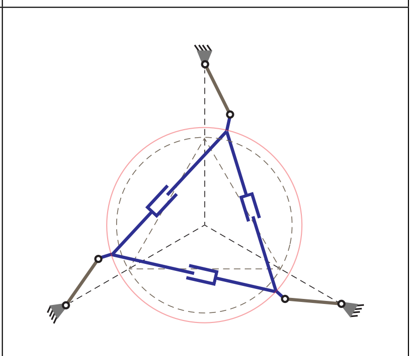
	Negative dilation	Positive dilation	Positive dilation

Table 1: Influence of the parameter δ on the kinematics of the system.

2.3 The rotation-dilation coupled oscillator

In order for the rotation-dilation system to act as a mechanical oscillator, spring components must be added. One way of realizing this system is depicted in Fig. 6, where elastic elements have been added to all the joints of the system. Rotation springs are added to the pivot joints and linear springs are added to the sliders. This substitution applies to all the designs presented in this paper.

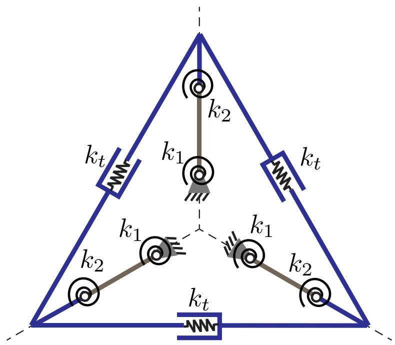

Figure 6: Kinematic diagram with elastic joints.

2.4 Generalization and particular cases

2.4.1 Particular case: $\delta = 0$

When $\delta = 0$, the connecting rods are attached to the ground at the center of the system and the size of the system stays constant as it rotates (no dilation).

2.4.2 Particular case: $\delta = -1$

This kinematics illustrated in Fig. 7 correspond conceptually to the case where $\delta = -1$, i.e., d and L are of opposite sign and go to infinity. It is noted that circular motion becomes straight line motion when the radius goes to infinity. This straight line motion can be implemented by replacing the pivots that attach the connecting rods to the ground by sliders with axis tangential to a circle with center O. The figure is the same for cases (b) and (c) of Fig. 4. Note that since $\delta < 0$, the dilation of this system is positive.

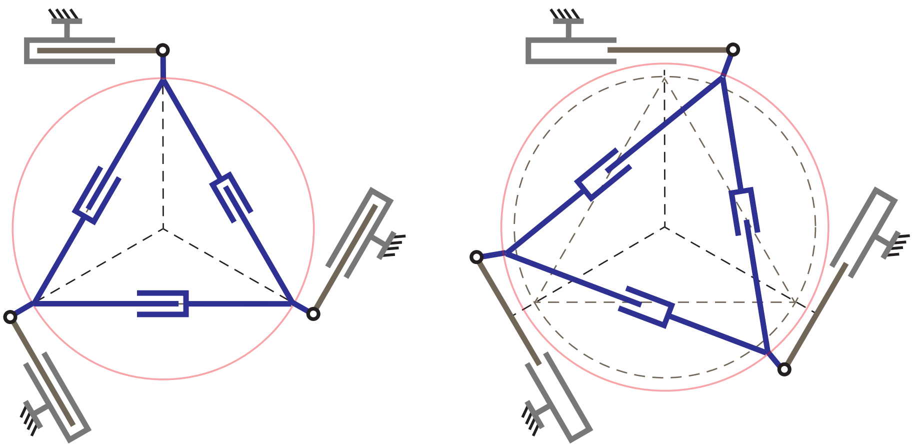

(a) Nominal position (b) Rotated

Figure 7: Translational RDCO ($\delta = -1$).

2.4.3 Increased order of symmetry

The system described in Sec. 2.1 can be realized with any order of rotational symmetry $n \geqslant 3$. The order n of the rotational symmetry corresponds to the number of inertial bodies and connecting rods. Fig. 8 shows variants with $n = 3$ to 5.

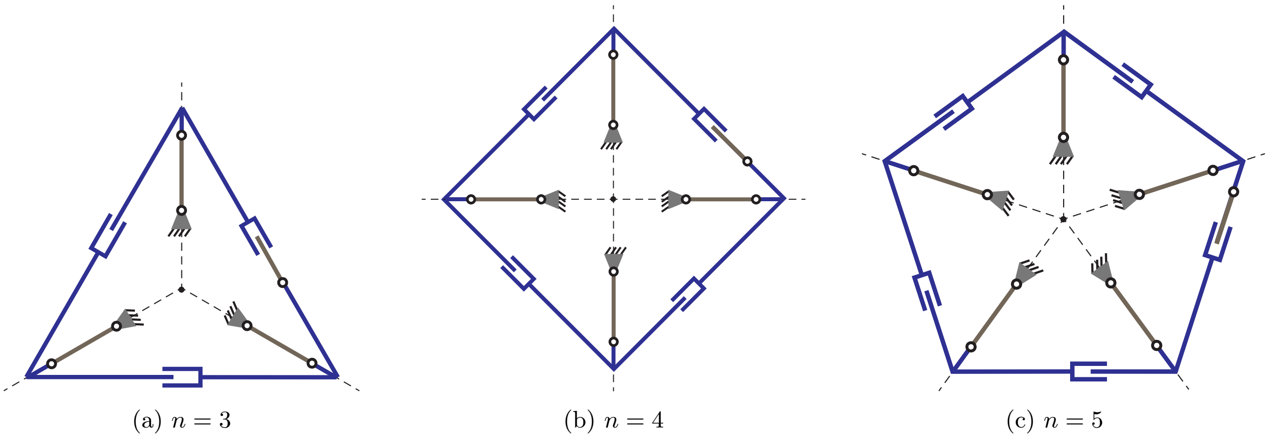

Figure 8: RDCO with different orders of symmetry.

2.5 Gravity sensitivity

Besides isochronism, a second crucial property for accurate timekeeping with mechanical watch time bases is gravity insensitivity: the independence of oscillation period from the orientation of the system with respect to gravity. The loading of flexures can be influenced by gravity, which changes their stiffness and causes variations of the period of the time base. This issue is not treated in this paper but it is known that symmetry of the system reduces its sensitivity to gravity [12]. We thus assume that the rotational symmetry of the RDCO will allow it to perform well under varying gravity orientation.

3 Flexure implementation

3.1 Flexure equivalent for ideal joints

The RDCO depicted in Fig. 6 can be implemented physically by replacing the ideal kinematic joints with flexures. Flexures have the advantage of realizing both the bearing and spring function of the joints, having an extremely low friction and allowing monolithic fabrication. Figure 9 shows different flexure equivalents for the connecting rods [4]. The connecting rod a) can be implemented with a flexure beam b), or by replacing its pivots with notch flexure hinges c), joined cross spring pivots also known as cartwheel flexure hinges (d), crossed flexure pivots (e), remote center of compliance (RCC) flexure pivots (f), or a combination of the previous pivots (g). The sliders can be implemented with parallel flexures which are known to closely approximate a sliding motion [4].

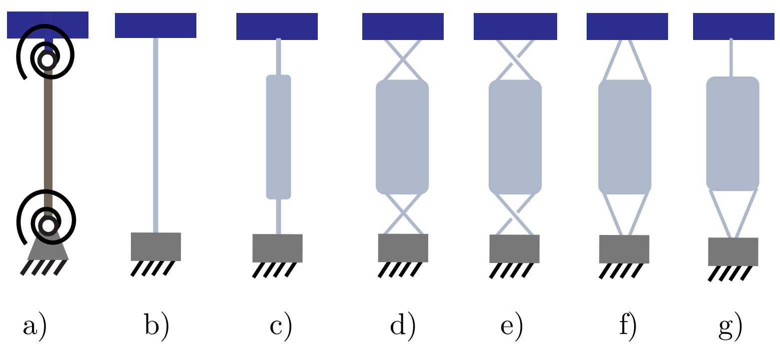

Figure 9: Flexure equivalents for the connecting rods.

3.2 Examples of flexure implementations

A wide range of variants arises from the combination of the designs described in Sec. 2 with the different flexure elements described in Fig. 9. They offer different properties and certain combinations can be particularly interesting, as will be discussed in Sec. 4.3. Figure 10 shows 4 examples. The connections to the ground are represented in orange. Note that in these designs, the extra DOF is omitted assuming that there is enough flexibility in the system to release the overconstraint.

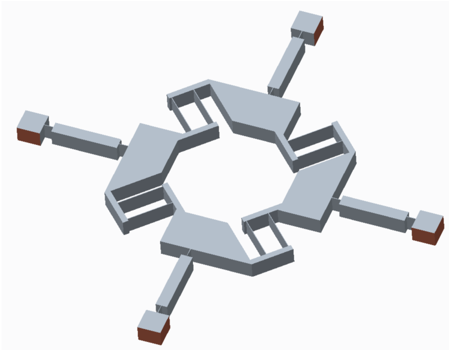

(a) $n = 4$, $\delta < -1$, notch hinges

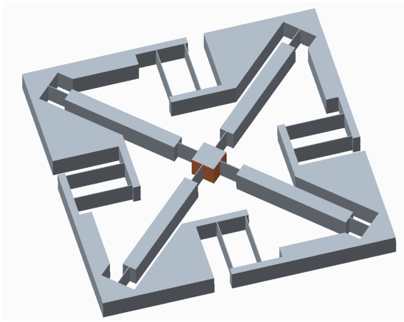

(b) $n = 4$, $\delta > 0$, notch hinges

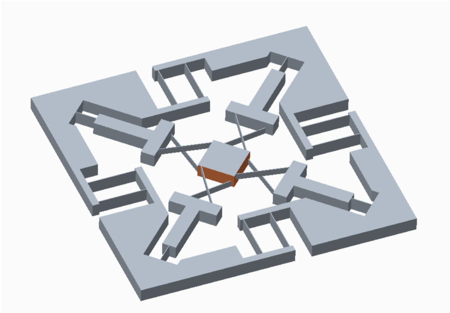

(c) $n = 4$, $\delta > 0$, notch hinge and crossed flexure pivot

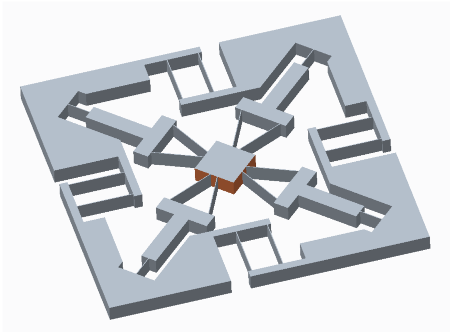

(d) $n = 4$, $\delta > 0$, notch hinge and RCC pivot

Figure 10: Examples of flexure implementations of the RDCO.

Figure 11 shows three ways of achieving the configuration with $-1 < \delta < 0$ (where the connecting rods cross each other in Table 1) while keeping the design planar. This can be of advantage for manufacturing and compactness. In designs 11a and 11b, the rigid part of the connecting rods is used to go around the attachment point of the other connecting rods. In design 11c, the remote center of rotation property of the RCC pivot is used to virtually place the pivot of the connecting rods on the other side of the center of the system O [4].

(a) $n = 4$, notch hinges

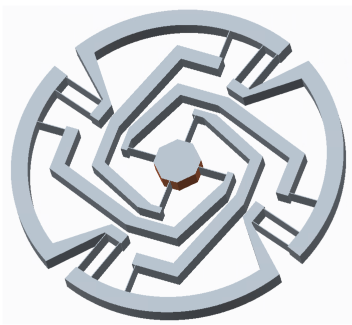

(b) $n = 4$, notch hinges

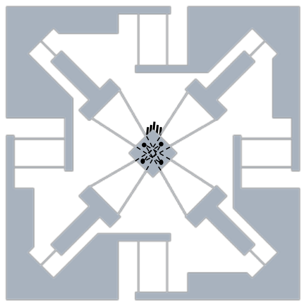

(c) $n = 4$, notch hinge and RCC pivot

Figure 11: Planar designs for the RDCO with $-1 < \delta < 0$.

4 Isochronism

4.1 Oscillation with varying inertia and nonlinear restoring torque

As explained in Sec. 1.3, the goal of this paper is to use the inertia variation of the oscillator in addition to its restoring torque nonlinearity to minimize its isochronism defect.

We consider the case of an oscillator whose restoring torque can be expressed by a power series having only odd terms (assuming the restoring torque to be antisymmetric with respect to equilibrium position)

$$M = k_0\,\theta(1+\mu\theta^2) + \mathcal{O}\left(\theta^5\right), \tag{1}$$

where k_0 is the *nominal stiffness* and μ the *relative restoring torque nonlinearity* [12], and whose inertia can be expressed by a power series having only even terms (assuming the inertia variation to be symmetric with respect to equilibrium position)

$$J = J_0\,\left(1+\iota\theta^2\right) + \mathcal{O}\left(\theta^4\right), \tag{2}$$

where J_0 is the *nominal inertia* and ι the *relative inertia variation.*

Solving the differential equation of this oscillator for small amplitudes around $\theta = 0$ using standard methods of perturbation theory [14, Eq. 2.3.34] yields the frequency-amplitude relation of the oscillator

$$\omega(\Theta) = \omega_0\left(1+\frac{3\,(\mu-\iota)}{8}\Theta^2\right) + \mathcal{O}\left(\Theta^4\right), \tag{3}$$

where Θ is the amplitude of oscillation and $\omega_0 = \sqrt{k_0/J_0}$ is the nominal frequency as amplitude approaches zero.

In order to be able to use Eq. (3) to minimize the dependence of oscillation frequency on amplitude, i.e. the isochronism defect, it is important to understand how to influence the sign of μ and ι. Table 1 shows how δ impacts the sign of the inertia variation (a positive dilation means $\iota > 0$ and a negative dilation $\iota < 0$) and the following section provides insight on the factors influencing the restoring torque nonlinearity μ of the system.

4.2 Restoring torque nonlinearity

We compute a simple analytical expression for the restoring torque nonlinearity of the RDCO. We assume that each flexure acts as a spring such as depicted in Fig. 6 and derive the restoring torque of an equivalent rotational spring using the strain energy of the system. We proceed with the following steps:

1. Derive the motion of the two pivots of the connecting rod for a given rotation of the oscillator.
2. Derive the motion of the sliders for a given rotation of the oscillator.
3. Express the strain energy of the system for a given rotation of the oscillator.
4. Compute the restoring torque of the system from its total strain energy and extract its relative nonlinearity.

We assume that the rotations are small and express terms using series expansions around $\theta = 0$.

4.2.1 Motion of the pivots of the connecting rod

The angles θ_1 and θ_2 swept by the pivots of the connecting rod when the system rotates by an angle θ can be obtained by trigonometry, see Fig. 12. They can be expressed using series expansions for small displacements:

$$\begin{aligned}\theta_2 &= \arcsin\frac{d\sin\theta}{L} = \delta\theta + \frac{1}{6}\delta\left(\delta^2-1\right)\theta^3 + \mathcal{O}\left(\theta^5\right)\\ \theta_1 &= \theta+\theta_2 = (1+\delta)\,\theta + \frac{1}{6}\delta\left(\delta^2-1\right)\theta^3 + \mathcal{O}\left(\theta^5\right).\end{aligned} \tag{4}$$

4.2.2 Motion of the sliders

The motion of the sliders corresponds to the change in distance s between the pivots of the inertial bodies, see Fig. 12. We first derive the distance from the center of the oscillator to these pivots as the oscillator rotates

$$r(\theta) = d\cos\theta + L\cos\theta_2 = L(\delta+1)\left(1-\frac{\delta}{2}\theta^2\right) + \mathcal{O}\left(\theta^4\right) = R_0\left(1-\frac{\delta}{2}\theta^2\right) + \mathcal{O}\left(\theta^4\right), \tag{5}$$

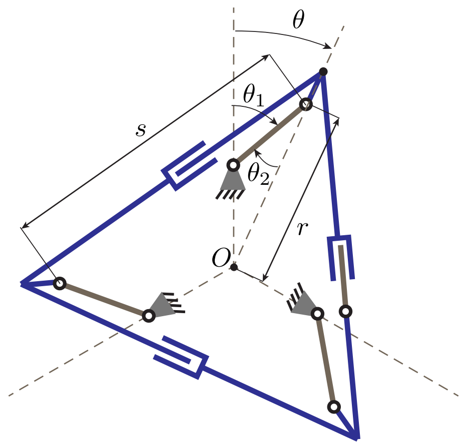

Figure 12: Parameters for the restoring torque computation.

where $R_0 = L + d$ in Fig. 5, from which we get the motion of the sliders

$$\Delta s(\theta) = s(\theta) - s(0) = 2\sin\frac{\pi}{n}\big(r(\theta) - r(0)\big) = -R_0\,\delta\sin\frac{\pi}{n}\theta^2 + \mathcal{O}\left(\theta^4\right). \tag{6}$$

We can see from these two equations that, as mentioned in Sec. 2.2, the sign of the dilation is the opposite of the sign of δ.

Remark. We express results in terms of R_0 instead of d or L as this parameter is more representative of the size of the oscillator and thus more convenient for dimensioning, see Fig. 5.

4.2.3 Strain energy

As labelled in Fig. 6, we call k_1 and k_2 the rotational stiffness of the pivots rotating by respectively θ_1 and θ_2, and k_t the linear stiffness of the slider. The strain energy of the system for a rotation θ is the sum of the strain energies of each elastic joint

$$U = n\left(\int_0^{\theta_1} k_1\,\beta\,d\beta + \int_0^{\theta_2} k_2\,\beta\,d\beta + \int_0^{\Delta s} k_t\,x\,dx\right), \tag{7}$$

which, when substituting with Eq. (4) and (6), yields

$$U = \frac{n}{2}\left((\delta+1)^2k_1 + \delta^2k_2\right)\theta^2 + \frac{n}{6}\delta\left((\delta+1)\left(\delta^2-1\right)k_1 + \delta\left(\delta^2-1\right)k_2 + 3\sin^2\left(\frac{\pi}{n}\right)\delta k_t R_0^2\right)\theta^4 + \mathcal{O}\left(\theta^6\right). \tag{8}$$

4.2.4 Restoring torque nonlinearity

The restoring torque for a rotation θ of the system is the derivative of the strain energy U with respect to θ

$$M = \frac{dU}{d\theta} = n\left((\delta+1)^2k_1 + \delta^2k_2\right)\theta + \frac{2n}{3}\delta\left((\delta+1)\left(\delta^2-1\right)k_1 + \delta\left(\delta^2-1\right)k_2 + 3\sin^2\left(\frac{\pi}{n}\right)\delta k_t R_0^2\right)\theta^3 + \mathcal{O}\left(\theta^5\right) \tag{9}$$

and the relative restoring torque nonlinearity according to Eq. (1) and neglecting the higher order terms is

$$\mu = \frac{2\delta\,(\delta+1)\left(\delta^2-1\right)k_1 + 2\delta^2\left(\delta^2-1\right)k_2 + 6\sin^2\left(\frac{\pi}{n}\right)\delta^2k_tR_0^2}{3\left((\delta+1)^2k_1 + \delta^2k_2\right)}. \tag{10}$$

The numerator of the restoring torque nonlinearity is a sum of three terms associated with the stiffness of each flexure element: k_1, k_2 and $k_tR_0^2$ (where k_t is multiplied by R_0^2 to be in comparable units). The sign of these terms depends on the value of δ and the sign of the nonlinearity μ of the system depends on δ and the relative weights of these three terms. Note that the sign of the denominator is always positive.

4.3 Conceptual example of isochronism defect minimization

Equation (3) explains how to use the contributions of ι and μ to set the isochronism defect of the RDCO. We now give a conceptual example of how the inertia variation and restoring torque nonlinearity can compensate each other to reach isochronism.

Our example focuses on architectures with order of symmetry $n = 3$ and small values of δ, which is convenient for compactness. This already allows to expose two types of solutions. The contributions of the three terms of the nonlinearity around $\delta = 0$ are plotted in Fig. 13. Note that the k_1 term is the only one that changes sign with δ and that it does it in the same way as ι, which is convenient for the desired compensating effect.

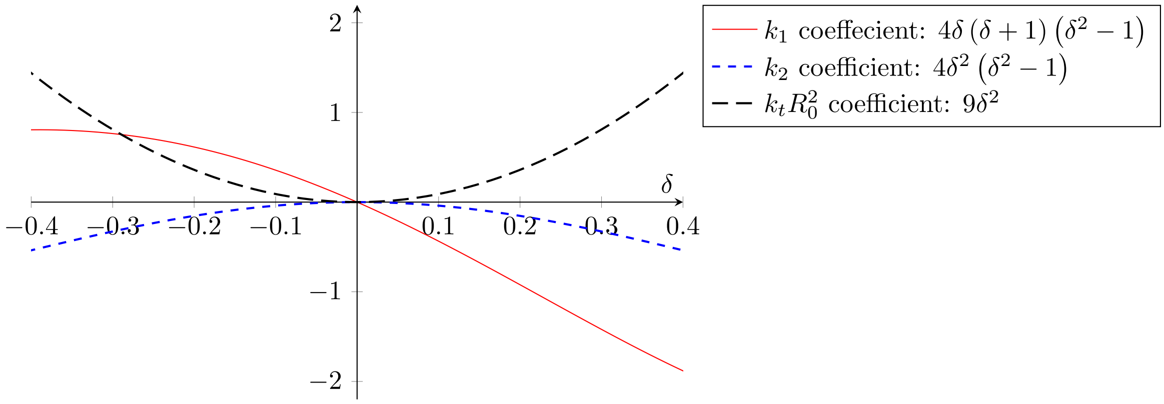

Figure 13: Effect of δ on the three terms forming the restoring torque nonlinearity.

Table 2 summarizes two configurations where the inertia and restoring torque defects can compensate each other:

a) The parameter δ is in the domain $-1 < \delta < 0$ and the positive dilation of the system ($\iota > 0$) compensates for the increasing stiffness of the system ($\mu > 0$). This stiffening occurs under the condition that the k_1 and $k_t R_0^2$ terms dominate the k_2 term in Eq. (10). This solution can be implemented such as depicted in Fig. 11a-11b.

b) The parameter δ is in the domain $0 < \delta < 1$ and the negative dilation of the system ($\iota > 0$) compensates for the decreasing stiffness of the system ($\mu < 0$). This decreasing stiffness occurs under the condition that the k_1 and k_2 terms dominate the $k_t R_0^2$ term in Eq. (10). This solution can be implemented such as depicted in Fig. 10b.

	ι	k_1 term	k_2 term	$k_t R_0^2$ term	μ for isochronism
a) $-1 < \delta < 0$	+	+	−	+	+
b) $0 < \delta < 1$	−	−	−	+	−

Table 2: Sign of the terms influencing the isochronism for two example configurations.

5 Conclusion and future work

This article presents a new way of tuning the isochronism of a flexure-based mechanical time base by varying its inertia. It also describes a new family of flexure oscillators with varying inertia. We gave the conceptual elements necessary for the design of an isochronous RDCO; it is now a question of finding appropriate dimensions for the elements. This will allow us to provide explicit estimates for the reduced isochronism defect.

Our future work will consist in full analytical modelling of the RDCO, finding dimensions for a prototype reaching desired properties and experimental validation of isochronism.

References

[1] F. Barrot et al. "Un Nouveau Régulateur Mécanique Pour Une Réserve de Marche Exceptionnelle". In: *Actes de La Journée d'Etude de La Société Suisse de Chronométrie*. 2014, pp. 43–48. URL: https://www.ssc.ch/commande-de-documents/.

[2] D. A. Bateman. “Vibration Theory and Clocks”. In: *Horological Journal* 120-121 (seven parts July 1977 to January 1978).

[3] E. Beckett, Lord Grimthorpe. *A Rudimentary Treatise on Clocks, Watches and Bells*. 8th ed. London: Crosby Lockwood and Son, D. Van Nostrand Company, 1903. URL: `http://www.gutenberg.org/ebooks/17576`.

[4] F. Cosandier et al. *The Art of Flexure Mechanism Design*. Lausanne, Switzerland: EPFL Press, 2017.

[5] G. Di Domenico et al. “Timepiece Resonator Mechanism”. European pat. 3206089 (A1). The Swatch Group Research and Development Ltd. CIB: G04B17/04. Aug. 16, 2017. URL: `https://worldwide.espacenet.com/publicationDetails/biblio?FT=D&date=20170816&DB=&locale=en_EP&CC=EP&NR=3206089A1&KC=A1&ND=4`.

[6] G. Di Domenico et al. “Timepiece Resonator with Crossed Blades”. Pat. WO2016096677 (A1). The Swatch Group Research and Development Ltd. CIB: G04B17/04. June 23, 2016. URL: `https://worldwide.espacenet.com/publicationDetails/biblio?FT=D&date=20160623&DB=EPODOC&locale=en_EP&CC=WO&NR=2016096677A1&KC=A1&ND=4`.

[7] F. S. Eastman. *Flexure Pivots to Replace Knife Edges and Ball Bearings, an Adaptation of Beam-Column Analysis,* Engineering Experiment Station Series. Seattle, USA: University of Washington, 1935.

[8] M. Grübler. *Getriebelehre: Eine Theorie Des Zwanglaufes Und Der Ebenen Mechanismen*. Berlin Heidelberg: Springer-Verlag, 1917. ISBN: 978-3-662-32953-5. URL: `https://www.springer.com/gp/book/9783662329535` (visited on 04/25/2019).

[9] J.-L. Helfer, G. Di Domenico, and P. Winkler. “Timepiece Resonator Mechanism”. European pat. 3200029 (A1). ETA SA Manufacture Horlogère Suisse. CIB: G04B15/14; G04B17/04; G04B17/10. Aug. 2, 2017. URL: `https://worldwide.espacenet.com/publicationDetails/biblio?FT=D&date=20170802&DB=&locale=en_EP&CC=EP&NR=3200029A1&KC=A1&ND=5`.

[10] S. Henein and P. Schwab. “Isochronism Corrector for Clockwork Escapement and Escapement Provided with Such a Corrector”. U.S. pat. 8672536B2. Centre Suisse d’Electronique et Microtechnique CSEM SA. Mar. 18, 2014. URL: `https://patents.google.com/patent/US8672536B2/en?inventor=henein%2c&assignee=csem&oq=henein%2c+csem`.

[11] C. Huygens. *Horologium Oscillatorium [Latin with English Translation by Ian Bruce]*. URL: `http://www.17centurymaths.com/contents/huygenscontents.html` (visited on 02/19/2019).

[12] M. H. Kahrobaiyan et al. “Gravity-Insensitive Flexure Pivot Oscillators”. In: *Journal of Mechanical Design* 140.7 (May 11, 2018), pp. 075002–9. ISSN: 1050-0472. DOI: `10.1115/1.4039887`. URL: `http://dx.doi.org/10.1115/1.4039887`.

[13] R. J. Matthys. *Accurate Clock Pendulums*. OUP Oxford, June 3, 2004. 275 pp. ISBN: 978-0-19-151368-8.

[14] A. Nayfeh and D. Mook. *Nonlinear Oscillations*. Wiley, Jan. 1, 1979. ISBN: 978-0-471-12142-8. DOI: `10.1002/9783527617586`.

[15] P. Privat-Deschanel and A. Focillon. *Dictionnaire Général Des Sciences Théoriques et Appliquées*. Paris, France: Delagrave-Garnier, 1880.

[16] A. L. Rawlings. *The Science of Clocks & Watches*. Third and Revised Edition edition. Upton, UK: British Horological Institute, 1993. ISBN: 978-0-9509621-3-9.

[17] E. Thalmann, M. H. Kahrobaiyan, and S. Henein. “Flexure-Pivot Oscillator Restoring Torque Nonlinearity and Isochronism Defect”. In: ASME 2018 International Design Engineering Technical Conferences and Computers and Information in Engineering Conference. Vol. 5A. American Society of Mechanical Engineers, Aug. 26, 2018, V05AT07A013. DOI: `10.1115/DETC2018-85863`.

[18] I. Vardi. “Le facteur de qualité en horlogerie mécanique”. In: *Bulletin de la Société Suisse de Chronométrie* 75 (2014), p. 9. URL: `http://infoscience.epfl.ch/record/263995`.

[19] I. Vardi. “Mathematics, the Language of Watchmaking”. In: *Watch Around* 20 (2015), pp. 90–94. URL: `http://infoscience.epfl.ch/record/213702`.

[20] P. Woodward. *My Own Right Time: An Exploration of Clockwork Design*. Oxford University Press, 1995. 184 pp.